NATIONAL ADVISORY COMMITTEE FOR AERONAUTICS

REPORT No. 571

PRESSURE DISTRIBUTION OVER A RECTANGULAR AIRFOIL WITH A PARTIAL-SPAN SPLIT FLAP

By CARL J. WENZINGER and THOMAS A. HARRIS

1936

For sale by the Superintendent of Documents, Washington, D. C. - - - - - - - - - - - - - - Price 10 cents

AERONAUTIC SYMBOLS

1. FUNDAMENTAL AND DERIVED UNITS

	Symbol	Metric		English	
		Unit	Abbreviation	Unit	Abbreviation
Length	l	meter	m	foot (or mile)	ft. (or mi.)
Time	t	second	s	second (or hour)	sec. (or hr.)
Force	F	weight of 1 kilogram	kg	weight of 1 pound	lb.
Power	P	horsepower (metric)		horsepower	hp.
Speed	V	kilometers per hour	k.p.h.	miles per hour	m.p.h.
		meters per second	m.p.s.	feet per second	f.p.s.

2. GENERAL SYMBOLS

W, Weight $= mg$

g, Standard acceleration of gravity $= 9.80665$ m/s^2 or 32.1740 ft./sec.^{2}

m, Mass $= \frac{W}{g}$

I, Moment of inertia $= mk^2$. (Indicate axis of radius of gyration k by proper subscript.)

μ, Coefficient of viscosity

ν, Kinematic viscosity

ρ, Density (mass per unit volume)

Standard density of dry air, 0.12497 kg-m^{-4}-s^2 at 15° C. and 760 mm; or 0.002378 lb.-ft.$^{-4}$-sec.^{2}

Specific weight of "standard" air, 1.2255 kg/m^3 or 0.07651 lb./cu.ft.

3. AERODYNAMIC SYMBOLS

S, Area

S_w, Area of wing

G, Gap

b, Span

c, Chord

$\frac{b^2}{S}$, Aspect ratio

V, True air speed

q, Dynamic pressure $= \frac{1}{2}\rho V^2$

L, Lift, absolute coefficient $C_L = \frac{L}{qS}$

D, Drag, absolute coefficient $C_D = \frac{D}{qS}$

D_o, Profile drag, absolute coefficient $C_{D_o} = \frac{D_o}{qS}$

D_i, Induced drag, absolute coefficient $C_{D_i} = \frac{D_i}{qS}$

D_p, Parasite drag, absolute coefficient $C_{D_p} = \frac{D_p}{qS}$

C, Cross-wind force, absolute coefficient $C_C = \frac{C}{qS}$

R, Resultant force

i_w, Angle of setting of wings (relative to thrust line)

i_t, Angle of stabilizer setting (relative to thrust line)

Q, Resultant moment

Ω, Resultant angular velocity

$\frac{Vl}{\rho\mu}$, Reynolds Number, where l is a linear dimension (e.g., for a model airfoil 3 in. chord, 100 m.p.h. normal pressure at 15° C., the corresponding number is 234,000; or for a model of 10 cm chord, 40 m.p.s. the corresponding number is 274,000)

C_p, Center-of-pressure coefficient (ratio of distance of $c.p.$ from leading edge to chord length)

α, Angle of attack

ϵ, Angle of downwash

α_o, Angle of attack, infinite aspect ratio

α_i, Angle of attack, induced

α_a, Angle of attack, absolute (measured from zero-lift position)

γ, Flight-path angle

REPORT No. 571

PRESSURE DISTRIBUTION OVER A RECTANGULAR AIRFOIL WITH A PARTIAL-SPAN SPLIT FLAP

By CARL J. WENZINGER and THOMAS A. HARRIS
Langley Memorial Aeronautical Laboratory

78659—36

NATIONAL ADVISORY COMMITTEE FOR AERONAUTICS

HEADQUARTERS, NAVY BUILDING, WASHINGTON, D. C.

LABORATORIES, LANGLEY FIELD, VA.

Created by act of Congress approved March 3, 1915, for the supervision and direction of the scientific study of the problems of flight (U. S. Code, Title 50, Sec. 151). Its membership was increased to 15 by act approved March 2, 1929. The members are appointed by the President, and serve as such without compensation.

TECHNICAL COMMITTEES

AERODYNAMICS
POWER PLANTS FOR AIRCRAFT
AIRCRAFT STRUCTURES AND MATERIALS
AIRCRAFT ACCIDENTS
INVENTIONS AND DESIGNS

Coordination of Research Needs of Military and Civil Aviation

Preparation of Research Programs

Allocation of Problems

Prevention of Duplication

Consideration of Inventions

LANGLEY MEMORIAL AERONAUTICAL LABORATORY

LANGLEY FIELD, VA.

Unified conduct, for all agencies, of scientific research on the fundamental problems of flight.

OFFICE OF AERONAUTICAL INTELLIGENCE

WASHINGTON, D. C.

Collection classification, compilation, and dissemination of scientific and technical information on aeronautics.

REPORT No. 571

PRESSURE DISTRIBUTION OVER A RECTANGULAR AIRFOIL WITH A PARTIAL-SPAN SPLIT FLAP

By Carl J. Wenzinger and Thomas A. Harris

SUMMARY

Pressure-distribution tests of a Clark Y wing model with a partial-span split flap were made to determine the distribution of air loads over both the wing and the flap. The model was used in conjunction with a reflection plane in the N. A. C. A. 7- by 10-foot wind tunnel. The 20-percent-chord split flap extended over the inboard 60 percent of the semispan. The tests were made at various flap deflections up to 45° and covered a range of angles of attack from zero lift to approximately maximum lift for each flap deflection.

The results are given as airfoil section, or rib, pressure diagrams for the wing with flap neutral. Increments of airfoil section pressures are given for various amounts of flap deflection so that combined wing and flap section pressure diagrams may be obtained by a simple addition. Calculated coefficients of section loads and moments and of wing loads and moments are also given for the wing and flap combination and for the flap alone.

It was found that deflecting a partial-span split flap affected the pressures and the section normal-force and pitching-moment coefficients over the entire wing span. The flap loads and moments were almost constant over the span of the partial-span flap for a given angle of attack and flap deflection. The maximum normal-force and hinge-moment coefficients were about the same for the partial-span split flap of the present tests as for a full-span split flap previously tested.

INTRODUCTION

A considerable amount of aerodynamic and air-load data is available for simple split flaps extending along the entire span of the wing. (See references 1 to 3.) However, because of the general use on present-day airplanes of the outer portion of the wing span for ailerons, most of the installations of split flaps have been limited to the inner 40 to 60 percent portion of the wing span. Some aerodynamic information on partial-span split flaps is available from wind-tunnel force tests of both rectangular and tapered wings equipped with such flaps (references 4 and 5). There are available, however, very few air-load and moment data suitable for the design of wings with partial-span split flaps.

The present investigation was made to obtain information, particularly of span load distribution, that would be suitable for application to design problems involving partial-span split flaps. The data were obtained from pressure-distribution tests of a wing model with a 20-percent-chord split flap in the N. A. C. A. 7- by 10-foot wind tunnel. The results are given as

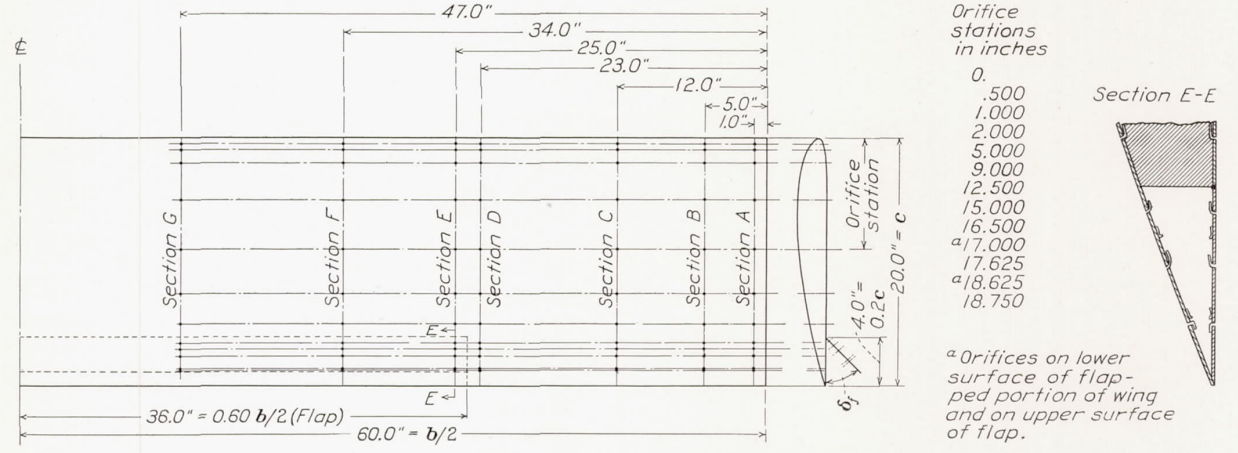

FIGURE 1.—Diagrammatic drawing of semispan Clark Y airfoil with split flap showing pressure orifices.

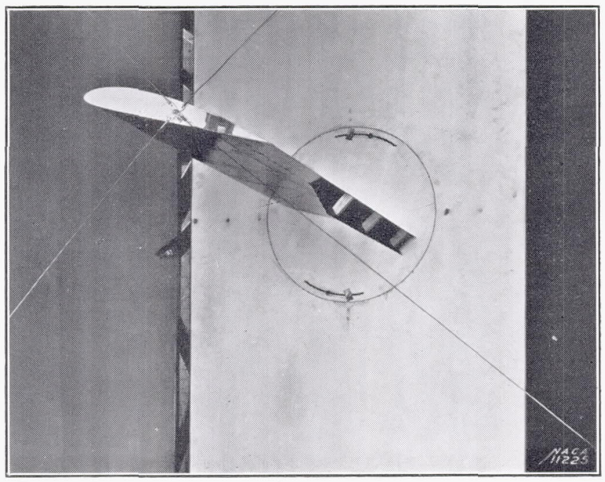

FIGURE 2.—Side view of model in tunnel.

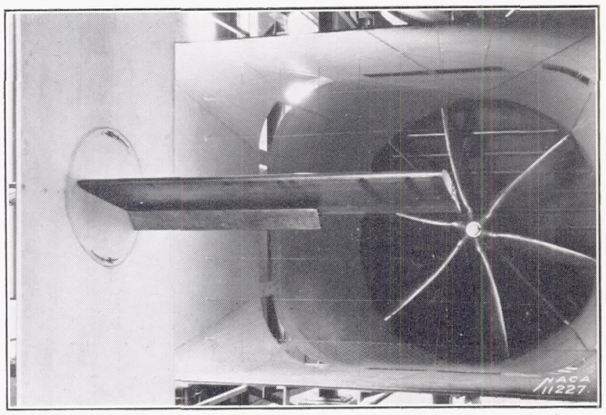

FIGURE 3.—Front view of model in tunnel.

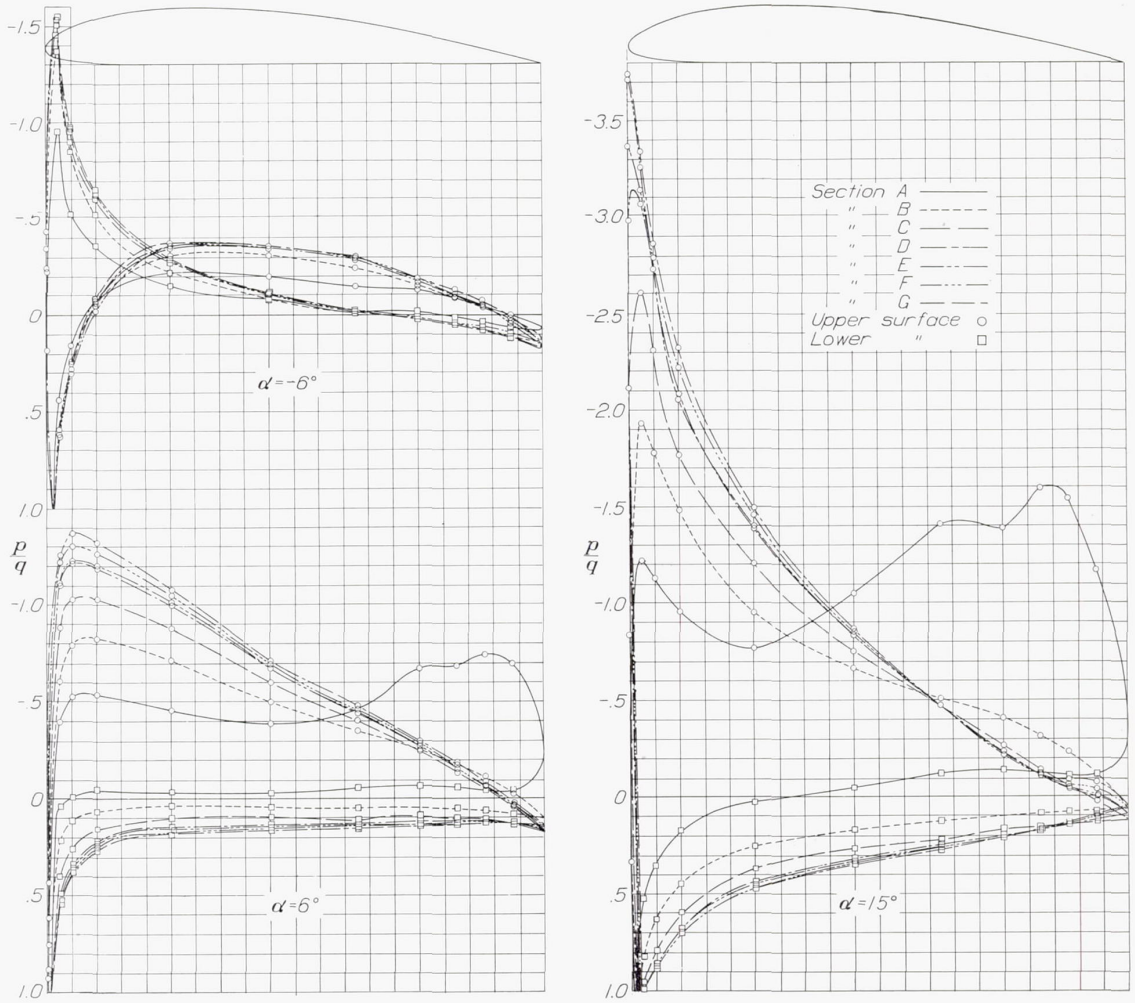

FIGURE 4.—Pressure distribution over airfoil sections at three angles of attack; $\delta_f = 0°$.

pressure diagrams for the basic wing and as increments in pressure or load for the flap-deflected conditions. The characteristics are given for the wing-and-flap combination and for the flap alone.

MODEL AND APPARATUS

WING MODEL

The Clark Y wing used for these tests had a 20-inch chord and a 60-inch semispan (fig. 1); the portion extending back to 80 percent of the wing chord was constructed of laminated mahogany. The trailing-edge, upper portion was constructed of $\frac{1}{16}$-inch-thick steel plate rolled to the contour and attached to the wooden part of the wing with screws. The flap, which had a 4-inch chord and a 36-inch semispan (20 percent c by 60 percent $b/2$), was formed by hinging the inboard 60 percent of the metal lower surface of the rear part of the wing about its leading edge. The flap was supported at its leading edge by small piano-type hinges and was set at the various deflections by suitable spacer blocks as shown in figure 2. The gap between the leading edge of the flap and the wing was sealed with plasticine for all tests.

Pressure orifices were built into the upper and lower surface of both the wing and flap at several sections along the semispan, 166 individual pressure orifices being installed. The tubes from the orifices were brought through the model and out at the inboard end. Two orifices on both the upper surface of the flap and on the lower surface of the wing at sections E, F, and G (fig. 1) were used to obtain the pressures between the flap and the wing.

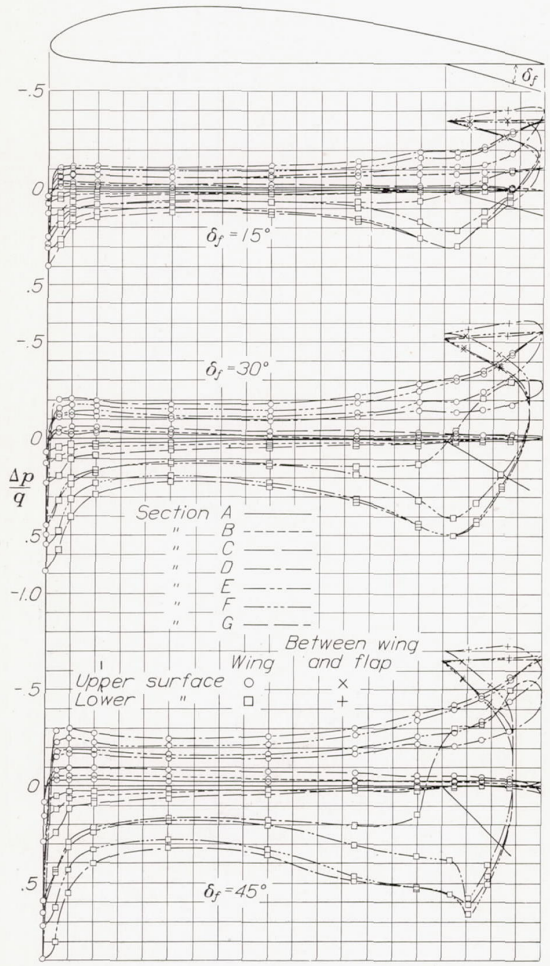

FIGURE 5.—Increments of pressure over airfoil sections at −6° angle of attack with the flap deflected various amounts.

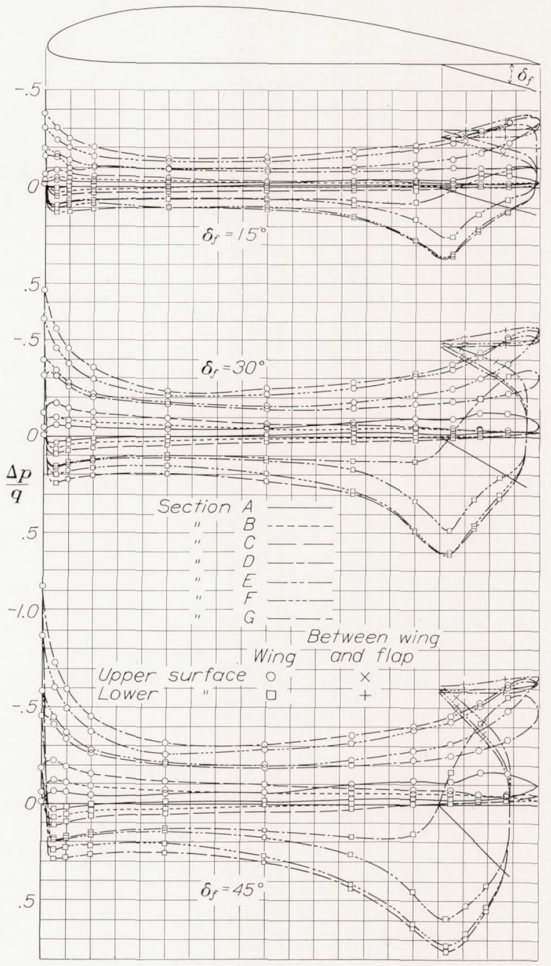

FIGURE 6.—Increments of pressure over airfoil sections at 6° angle of attack with the flap deflected various amounts.

MANOMETERS

Two N. A. C. A. multiple-tube photographic-recording manometers (described in reference 6) were used to record the point pressures on the model. The manometer was connected to the orifices by means of rubber tubing, so arranged as not to affect the air flow over the wing.

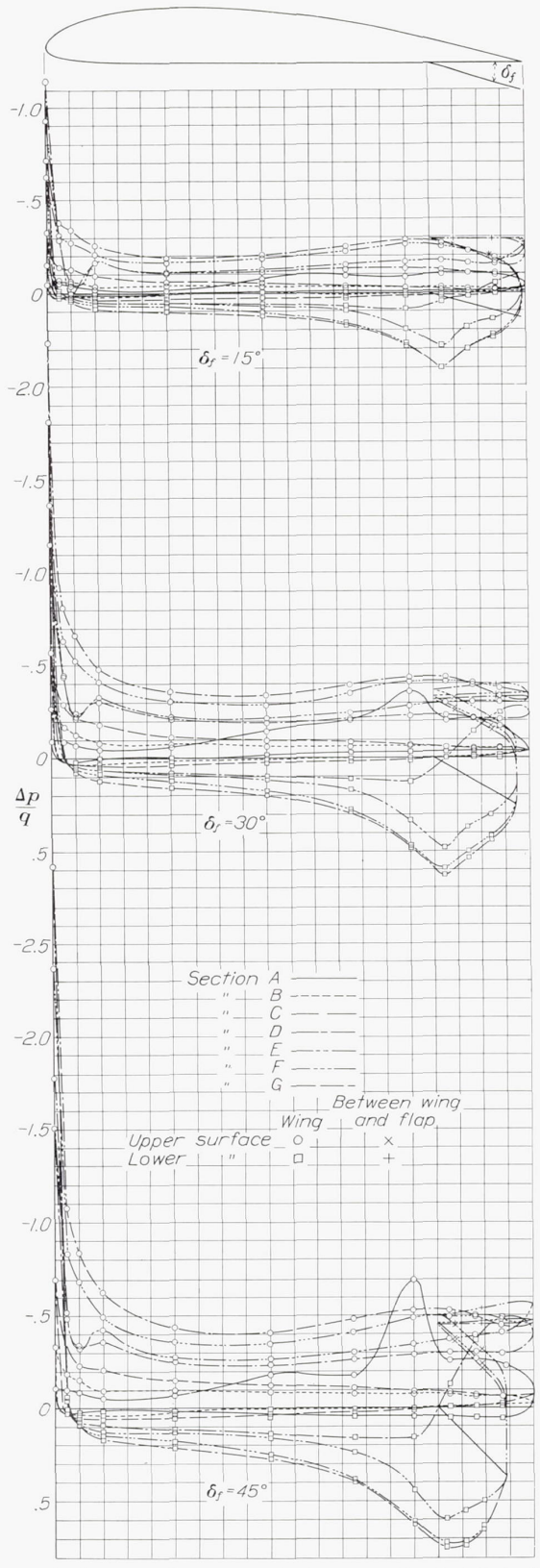

FIGURE 7.—Increments of pressure over airfoil sections at 15° angle of attack with the flap deflected various amounts.

TEST ARRANGEMENT

The model was mounted in the N. A. C. A. 7- by 10-foot wind tunnel (reference 7) in conjunction with a reflection plane at the inboard end. (See figs. 2 and 3). This plane extended from the top to the bottom of the air stream and some distance ahead of and behind the model and was so located that the model was placed symmetrically with respect to the tunnel center line. The tubes from the pressure orifices were brought horizontally through a rotatable section of this plane to the edge of the jet and were grouped together to form a streamline shape so that the air flow on the opposite side of the plane, on which the model was located, was not appreciably disturbed.

TESTS

The static reference pressure used to maintain the dynamic pressure constant during the tests was calibrated against dynamic-pressure surveys at the model location with the model removed from the tunnel. The longitudinal static pressure at the model location was also measured and used to correct the point pressures to the correct reference pressure.

All the tests were made at a dynamic pressure of 16.37 pounds per square foot, corresponding to an air speed of 80 miles per hour under standard sea-level atmospheric conditions. The average Reynolds Number of the tests, based on the wing chord, was approximately 1,220,000.

The model was tested with flap angles of 0°, 15°, 30°, and 45°. The angles of attack covered a range from approximately zero lift to 15° (approximately $C_{L_{max}}$) with each flap setting, test points being taken at 3° intervals. When the model had been fixed at a given angle of attack with a given flap setting, a few minutes were allowed for conditions to become constant; a record was then taken of the pressures at the orifices by means of the photographic manometer.

PRESENTATION OF DATA

Section or rib pressure diagrams with the flap neutral (fig. 4) are given as ratios of point pressure p to dynamic pressure q for a low angle of attack ($-6°$), an intermediate angle of attack (6°), and a high angle of attack (15°). In addition to the section pressure diagrams with the flap neutral, the increments of point pressure with the flap deflected over the point pressure with the flap neutral (both in terms of the dynamic pressure) are given (figs. 5 to 7) for all flap deflections and for the three previously mentioned angles of attack. On these diagrams the flap pressures are plotted from the deflected flap chord but normal to the wing chord. The principal advantage of the increment diagrams is that they may, by the principle of superposition, be applied to pressure diagrams of any other basic wing section that does not depart too greatly from the Clark Y section of which the tests were made.

The data computed from the integrated pressure diagrams are given as nondimensional coefficients. The coefficients for the wing-and-flap combination include the loads of the flap projected onto the wing chord. The coefficients are defined as follows:

$c_{n_w}=\frac{n_w}{qc_w}$, airfoil section normal-force coefficient.

$C_{m_{c/4}}=\frac{M_{w_{c/4}}}{qc_w{}^2b_w}$, wing pitching-moment coefficient about quarter-chord point.

$c_{h_f}=\frac{h_f}{qc_f{}^2}$, flap section hinge-moment coefficient about flap hinge.

$C_{h_f}=\frac{H_f}{qc_f{}^2b_f}$, flap hinge-moment coefficient about flap hinge.

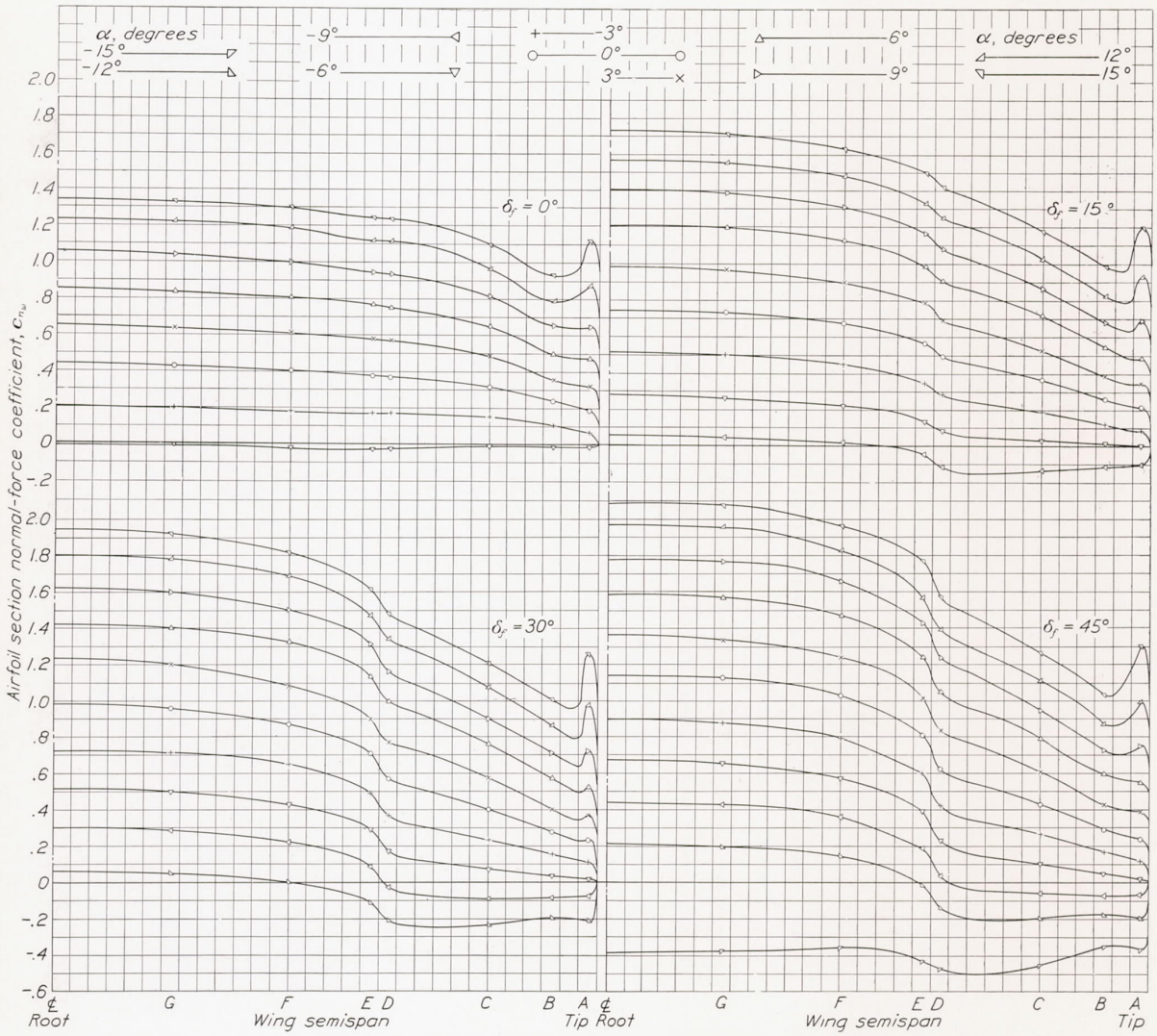

FIGURE 8.—Span load distribution on the airfoil with the flap deflected various amounts.

$C_{N_w}=\frac{N_w}{qc_wb_w}$, wing normal-force coefficient.

$c_{n_f}=\frac{n_f}{qc_f}$, flap section normal-force coefficient.

$C_{N_f}=\frac{N_f}{qc_fb_f}$, flap normal-force coefficient.

$c_{m_{c/4}}=\frac{m_{w_{c/4}}}{qc_w{}^2}$, airfoil section pitching-moment coefficient about quarter-chord point.

$(c.\ p.)_w=\left(0.25-\frac{c_{m_{c/4}}}{c_{n_w}}\right)\times 100$, airfoil section longitudinal center of pressure in percentage of wing chord from wing leading edge.

$(C.\ P.)_w=\left(0.25-\frac{C_{m_{c/4}}}{C_{N_w}}\right)\times 100$, wing center of pressure in percentage of wing chord from wing leading edge.

$(c.\ p.)_f = \left(-\frac{c_{h_f}}{c_{n_f}}\right) \times 100$, flap section center of pressure in percentage of flap chord from hinge.

$(C.\ P.)_f = \left(-\frac{C_{h_f}}{C_{N_f}}\right) \times 100$, flap center of pressure in percentage of flap chord from hinge.

$(C.\ P.)_{w_{lat}} = \left(\frac{M_{w_{lat}}}{\frac{N_w b_w}{4}}\right) \times 100$, wing lateral center of pressure in percentage of wing semispan from wing root.

$M_{w_{c/4}}$, wing pitching moment about the quarter-chord point.

h_f, flap section hinge moment per unit span about the flap hinge.

H_f, flap hinge moment about the flap hinge.

$M_{w_{lat}}$, moment of wing semispan load about wing root.

$M_{f_{lat}}$, moment of flap semispan load about inboard end of flap.

q, dynamic pressure.

c_w, wing chord.

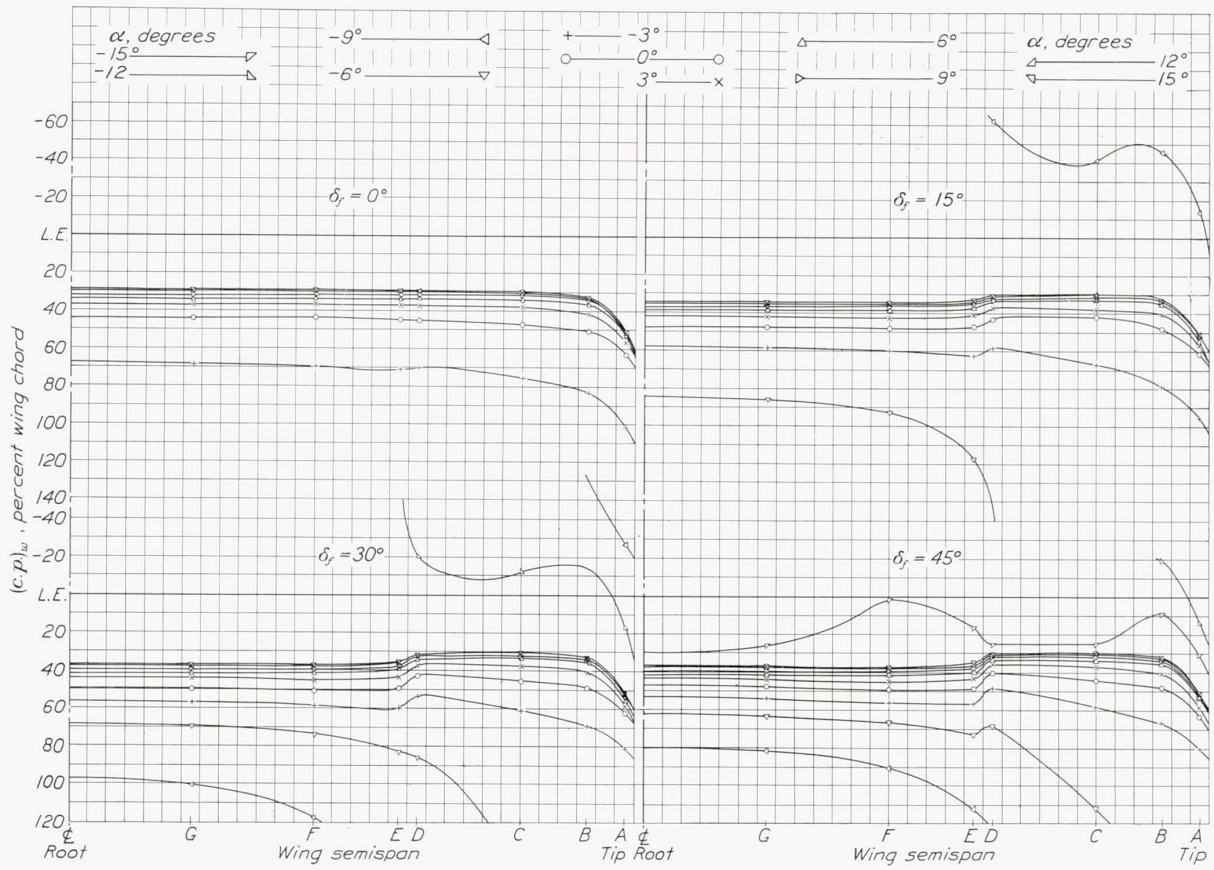

FIGURE 9.—Airfoil section longitudinal centers of pressure against span of wing with the flap deflected various amounts.

$(C.\ P.)_{f_{lat}} = \left(\frac{M_{f_{lat}}}{\frac{N_f b_f}{4}}\right) \times 100$, flap lateral center of pressure in percentage of flap semispan from inboard end of flap.

where

n_w is the airfoil section normal force per unit span.

N_w, wing normal force.

n_f, flap section normal force per unit span.

N_f, flap normal force.

$m_{w_{c/4}}$, airfoil section pitching moment per unit span about the quarter-chord point.

c_f, flap chord.

b_w, wing span.

b_f, flap span.

In these coefficients it is to be noted that the chord forces on the airfoil have been neglected; i. e., the longitudinal center-of-pressure positions and the pitching-moment coefficients were derived solely from considerations of the normal forces.

The airfoil section normal-force coefficients are plotted against the wing semispan in figure 8 for all flap deflections and all angles of attack tested. The

airfoil section centers of pressure are plotted similarly in figure 9. In addition to these data, the increments of airfoil section normal-force and pitching-moment coefficients, Δc_n and Δc_m, for the three angles of attack previously mentioned are given in figure 10. The airfoil section coefficients c_n and c_m are also plotted against angle of attack for all the flap deflections in figure 11. The wing normal-force and pitching-moment coefficients and longitudinal centers of pressure are plotted against angle of attack for all flap deflections in figure 12, and the wing lateral centers of pressure are given for all flap deflections in figure 13.

The flap section normal-force coefficients are plotted against flap semispan in figure 14 for all flap deflections and angles of attack. It should be noted that for $\delta_f = 0°$ the coefficients were computed for the load on only the lower surface of the flap, whereas for the other flap deflections the coefficients include the loads on both the upper and lower surfaces of the flap. This condition also applies to the flap centers of pressure and hinge-moment coefficients. The flap section centers of pressure for all flap deflections and angles of attack are plotted against flap semispan in figure 15. The flap normal-force and hinge-moment coefficients and longitudinal centers of pressure are plotted against wing normal-force coefficients in figure 16 for all flap deflections and angles of attack. The flap lateral centers of pressure are plotted against angle of attack in figure 17.

PRECISION

Inasmuch as no air-flow alinement tests were made in the wind tunnel with the test arrangement used for this investigation, the absolute setting of the angle of attack may be slightly in error; the relative angles are, however, accurate to within $\pm 0.1°$. The flap deflections were set to the specified angles to within $\pm 0.1°$. The point pressures based on check tests in which both the angle of attack and the flap settings were changed independently showed that they agreed to within ± 2 percent, with the exception of the upper-surface pressures near the wing leading edge which, at high angles of attack, checked to within ± 5 percent. The dynamic pressure recorded on each diagram was accurate to within ± 0.25 percent for all tests. Since the dynamic pressure was recorded on each diagram, there is no relative error between it and the point pressure; therefore variations of the dynamic pressure do not introduce any error in computing the coefficients. None of the data has been corrected for the effects of the jet boundaries.

RESULTS AND DISCUSSION

SECTION PRESSURE DISTRIBUTION

The distribution of pressure over the airfoil sections with the flap neutral (fig. 4) is typical of that for wings of rectangular plan form. The expected high tip

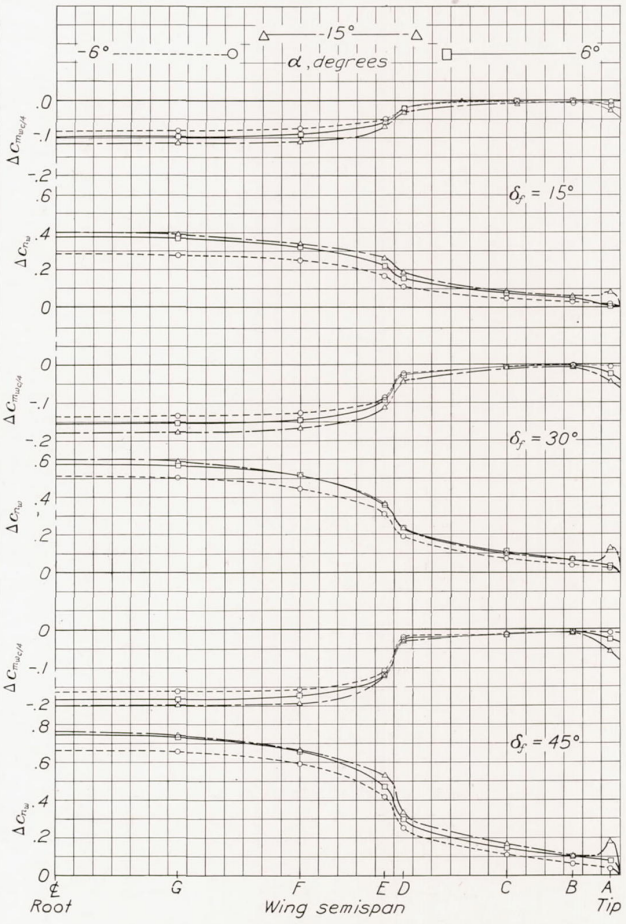

FIGURE 10.—Increments in airfoil section normal-force and pitching-moment coefficients with the flap deflected various amounts.

loads at the high angle of attack verify previous conclusions that structurally the rectangular tip shape is poor. The data for angles of attack other than those shown were not believed to be of sufficient general interest to include in this report.

The increments of pressure due to the deflected flap at the low angle of attack, $-6°$, (fig. 5) show that the partial-span flap affects the load distribution on all sections along the span of the wing. The first section outboard of the tip of the flap, section D, shows a

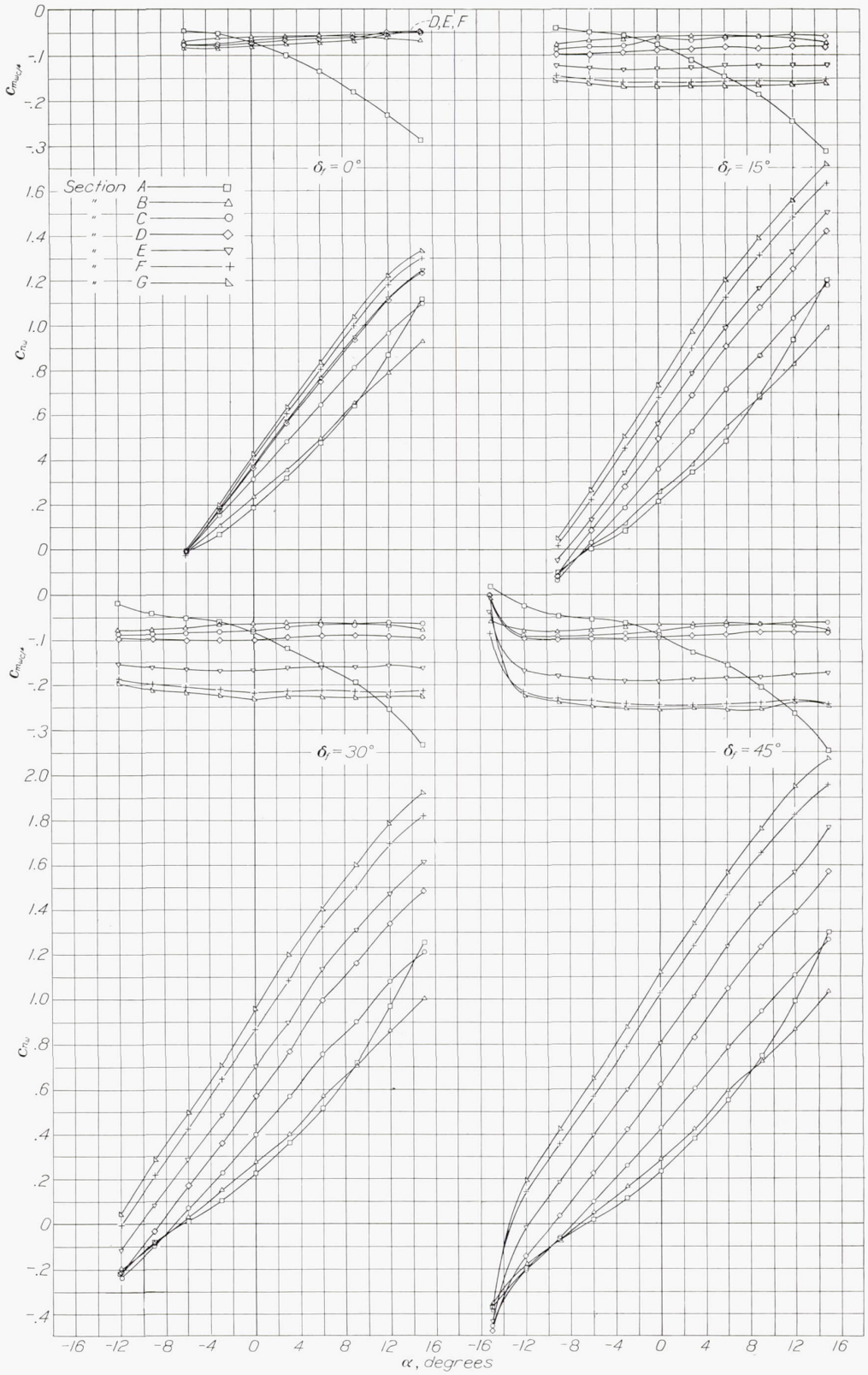

FIGURE 11.—Airfoil section normal-force and pitching-moment coefficients with the flap deflected various amounts.

peculiar resultant down-load increment at the trailing edge of the wing, which increases as the flap is deflected downward. There is also a considerable resultant down-load increment on the trailing-edge portion of the wing covered by the flap when the flap is deflected, which increases with flap deflection. In addition, the positive pressures on the lower surface of the wing are

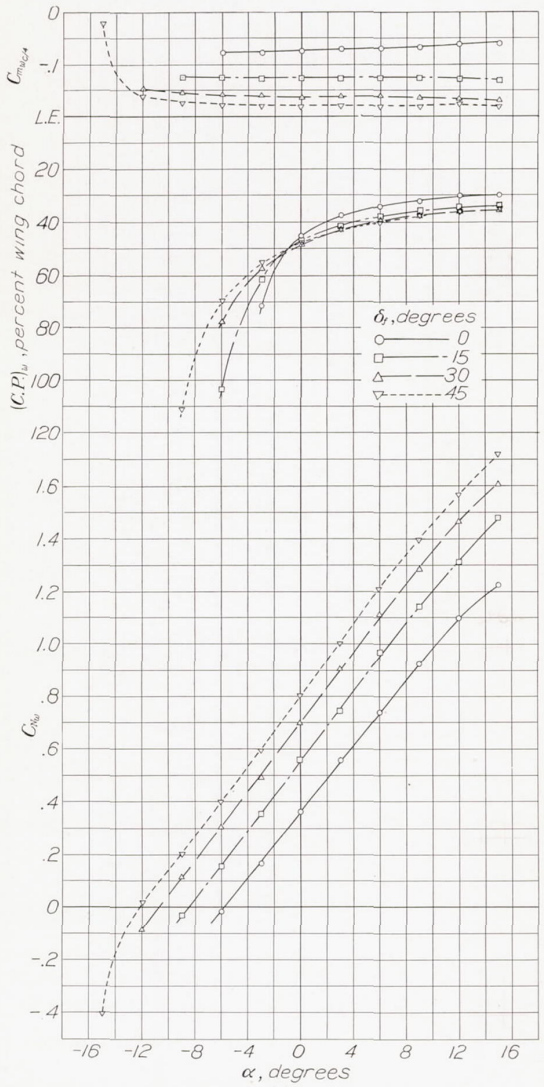

FIGURE 12.—Normal-force coefficients, pitching-moment coefficients, and centers of pressure of the wing with the flap deflected various amounts.

increased more than the negative pressures on the upper surface at a given flap deflection. The pressures are increased the greatest amount near the flap hinge and near the leading edge of the wing.

At the intermediate angle of attack, 6° (fig. 6), there is a peculiar increase in load at the tip of the wing, which is probably a function of the wing plan as well as of the flap deflection. The increments of pressure at the trailing edge of the wing are quite similar to those noted for the low angle of attack. In addition, the increase in positive pressure near the flap hinge on the lower surface of the wing is larger. This increase in load near the hinge may be critical in rib design because normally this portion of the rib does not have large loads. The negative pressure on the upper surface near the leading edge increases at this angle of attack by about 75 percent of the dynamic pressure with the maximum flap deflection.

At an angle of attack of 15° (fig. 7) the increase in load on the tip section is again evident. At this angle of attack the resultant down-load increment near the trailing edge at section D with the flap down is less than for the lower angles of attack. The load increment on the portion of the wing above the flap is very small but the increment on the wing outboard of the flap is large, increasing with flap deflection. The

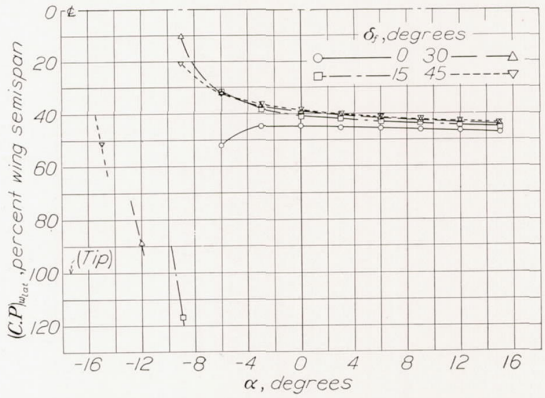

FIGURE 13.—Lateral centers of pressure of wing with the flap deflected various amounts.

large increase in positive pressure near the flap hinge is also evident and is in agreement with the results of the tests reported in reference 3. The increased negative pressure at the wing leading edge is about three times the dynamic pressure when the flap is fully deflected.

WING LOADS AND MOMENTS

The airfoil section normal-force coefficients plotted in figure 8 show the actual distribution of the air load along the span for all the angles of attack and the flap deflections tested. With the flap neutral, the span load distribution is typical of that for rectangular airfoils. With the flap deflected, the section normal-force coefficient increases along the entire span of the wing. The rapid change in section normal-force coefficients at the tip of the flap is very noticeable. The curves show that the larger the flap deflection, the greater is the concentration of the load over the flapped portion of the wing for a given total load. The high tip loads may be attributed to the particular plan form of the wing.

The section centers of pressure plotted against the span of the wing with the flap neutral (fig. 9) are

typical of those for a wing of rectangular plan form. The center of pressure moves forward as the angle of attack is increased and is nearly uniform over the span except at the tips of the wing, which may be seen from the pressure-distribution diagrams (fig. 4). With the flap deflected (fig. 9), the center of pressure shifts rearward not only over the flapped portion of the wing but also over the rest of the wing to the outboard end for the high angles of attack. For the low angles of attack, the center of pressure shifts forward over the unflapped portion of the wing when the flap is deflected.

The increments of airfoil section normal-force and pitching-moment coefficients caused by deflecting the flap (fig. 10) are probably of greater interest than the wing coefficients for a particular model. The largest changes in section normal-force coefficient, $\Delta c_n = 0.75$, and in section pitching-moment coefficient, $\Delta c_{m_{c/4}} = -0.20$, occur at the maximum flap deflection used and at 15° angle of attack. The rapid change in both the wing normal-force and pitching-moment coefficients at the outboard end of the flap and the increase in the force and moment on the unflapped portion of the wing are clearly shown by these increment diagrams. The peak load and moment increments at the tip of the wing are probably a function of the rectangular tip shape and might not be encountered with rounded wing tips. It is probable that these increments of loads and moments may safely be superposed on known span load and moment diagrams of plain wings having similar profiles and plan forms.

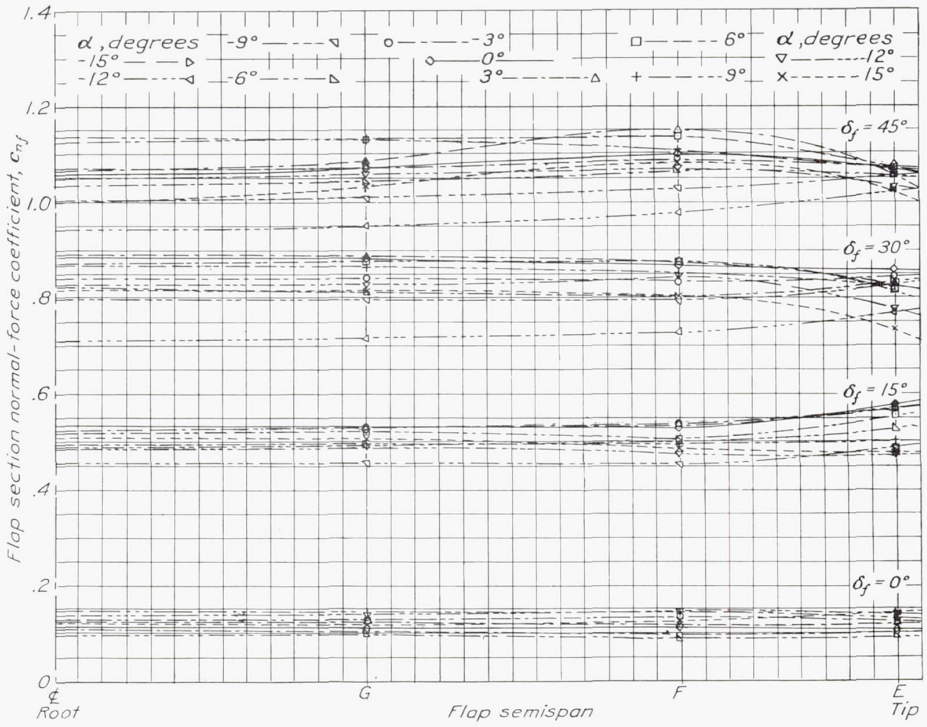

FIGURE 14.—Span load distribution on flap for various flap deflections.

In order to complete the air-load information on wings with this type of flap, more tests are desirable with other wing profiles and plan forms and flaps of different spans and chords. Such additional data would establish the effect of profile and plan form on section-characteristic increments and on span-load and moment increments.

The curves of the section normal-force coefficient (fig. 11) show that for all sections except A and B the normal-force coefficient is linearly proportional to the angle of attack from zero lift to 15° angle of attack. The pitching-moment coefficient curves, except for section A, are regular, the moment increasing toward the center of the wing. As previously pointed out, the peculiar loads and moments at the tip section are a function of the tip shape.

The variation in the wing characteristics with angle of attack (fig. 12), caused by deflecting the partial-span flap a given amount, checks reasonably well with the results of force tests (data unpublished). The sudden change in normal force at high negative angles of attack with the flap down 45° is worthy of note. The same phenomenon was encountered in force tests with split flaps (references 2 and 4) and may result in critical loads when considering a down gust if flying at maximum allowable speed with the flap deflected. More data on conditions in this vicinity are desirable.

The lateral center of pressure on the wing (fig. 13) moves toward the plane of symmetry as the flap is deflected downward.

FLAP LOADS AND MOMENTS

The flap section normal-force coefficients are shown in figure 14 for all flap deflections and angles of attack plotted against flap span. For the zero flap deflection the load on only the lower surface of the flap was considered, but for the other flap deflections the load on both surfaces was included. The section normal-force coefficient of the flap increases with flap deflection but shows no consistent variation with angle of attack. For practical purposes the air-load distribution may be considered uniform over the span of the flap.

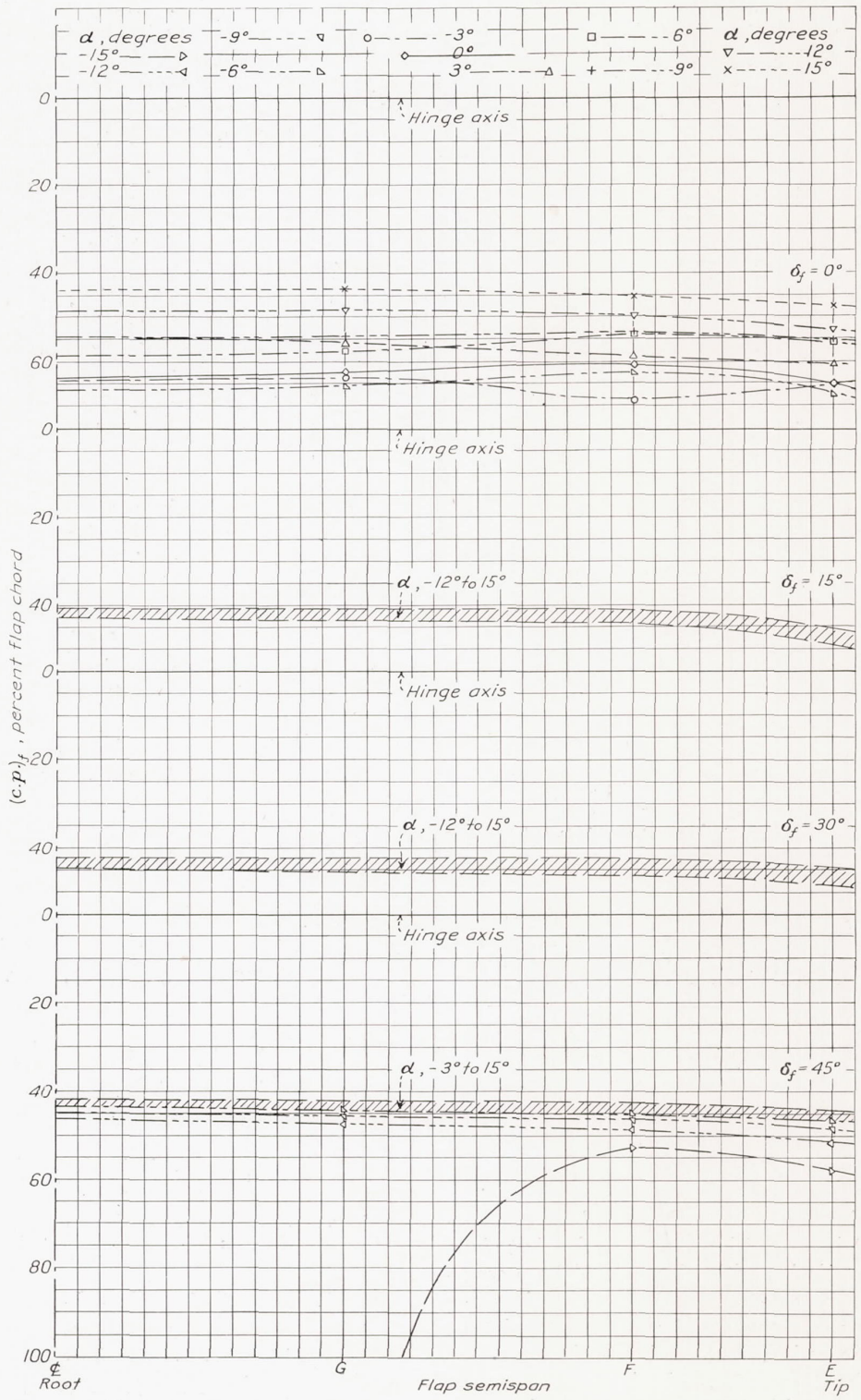

FIGURE 15.—Flap section longitudinal centers of pressure against span of flap for various flap deflections.

The flap section centers of pressure (fig.15) with the flap neutral are rather erratic and vary over a large range; for other flap deflections the flap center of pressure is essentially constant between 40 and 50 percent of the flap chord from the hinge axis.

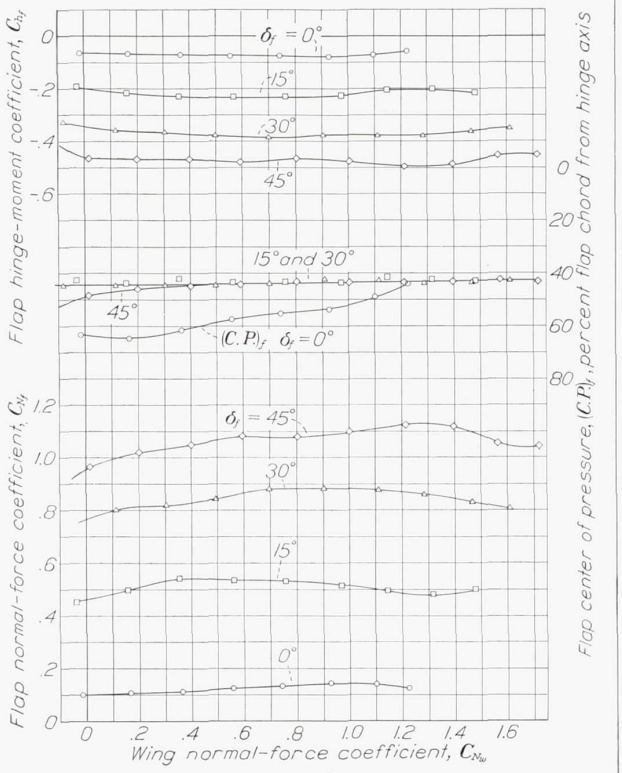

FIGURE 16.—Normal-force coefficients, hinge-moment coefficients, and centers of pressure of flap for various flap deflections.

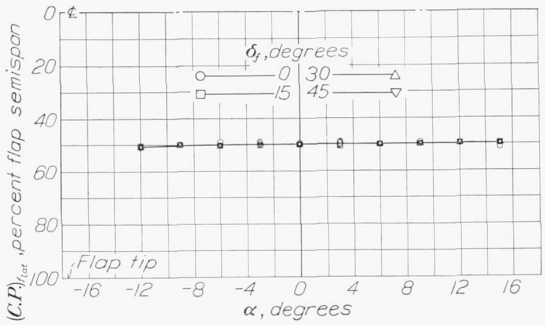

FIGURE 17.—Lateral centers of pressure of flap for various flap deflections.

The flap hinge-moment and normal-force coefficients (fig. 16) increase with flap deflection but show no consistent variation with wing normal-force coefficient. The maximum flap normal-force coefficient was 1.15, which checks the results of references 2 and 3 for the same flap deflection. The maximum hinge-moment coefficient of the flap was 0.5, which is about 10 percent less than that reported for the full-span flap of reference 2.

The longitudinal center of pressure on the flap (fig. 16) is about constant at 43 percent of the flap chord from the hinge axis except when the flap is neutral and for small values of the wing normal-force coefficient with the flap down 45°. With the flap neutral the center of pressure moves to about 65 percent of the flap chord at small values of wing normal-force coefficient. The lateral center of pressure on the flap (fig. 17) is at 50 percent of the flap span from the plane of symmetry, within ±0.5 percent, for all flap deflections and angles of attack tested.

The amount of leakage between the wing and a closed split flap largely determines the hinge-moment and normal-force coefficient for the neutral setting. If there is any negative pressure on the upper surface of the flap in the closed position, the hinge-moment and normal-force coefficients will be increased. It is possible that the force required to overcome the hinge moment when the flap is neutral may be critical for manual operation of the flap. Further tests of various flap-neutral conditions seem desirable.

CONCLUSIONS

The following conclusions may be drawn from the results of the tests reported herein:

1. Deflection of the partial-span split flap affected the pressures and section normal-force and pitching-moment coefficients over the entire span of the wing.
2. For the wing-flap combination tested, the flap loads and moments were practically constant over the span of the partial-span split flap for a given flap deflection and angle of attack of the wing.
3. The maximum normal-force and hinge-moment coefficients were about the same for the partial-span split flap of the present tests as for a previously tested full-span split flap.

LANGLEY MEMORIAL AERONAUTICAL LABORATORY,
NATIONAL ADVISORY COMMITTEE FOR AERONAUTICS,
LANGLEY FIELD, VA., *April 28, 1936.*

REFERENCES

1. Weick, Fred E., and Harris, Thomas A.: The Aerodynamic Characteristics of a Model Wing Having a Split Flap Deflected Downward and Moved to the Rear. T. N. No. 422, N. A. C. A., 1932.
2. Wenzinger, Carl J.: Wind-Tunnel Measurements of Air Loads on Split Flaps. T. N. No. 498, N. A. C. A., 1934.
3. Wallace, Rudolf: Investigation of Full-Scale Split Trailing-Edge Wing Flaps with Various Chords and Hinge Locations. T. R. No. 539, N. A. C. A., 1935.
4. Wenzinger, Carl J.: The Effect of Partial-Span Split Flaps on the Aerodynamic Characteristics of a Clark Y Wing. T. N. No. 472, N. A. C. A., 1933.
5. Wenzinger, Carl J.: The Effects of Full-Span and Partial-Span Split Flaps on the Aerodynamic Characteristics of a Tapered Wing. T. N. No. 505, N. A. C. A., 1934.
6. Parsons, John F.: Full-Scale Force and Pressure-Distribution Tests on a Tapered U. S. A. 45 Airfoil. T. N. No. 521, N. A. C. A., 1935.
7. Harris, Thomas A.: The 7 by 10 Foot Wind Tunnel of the National Advisory Committee for Aeronautics. T. R. No. 412, N. A. C. A. ,1931.

U. S. GOVERNMENT PRINTING OFFICE: 1936

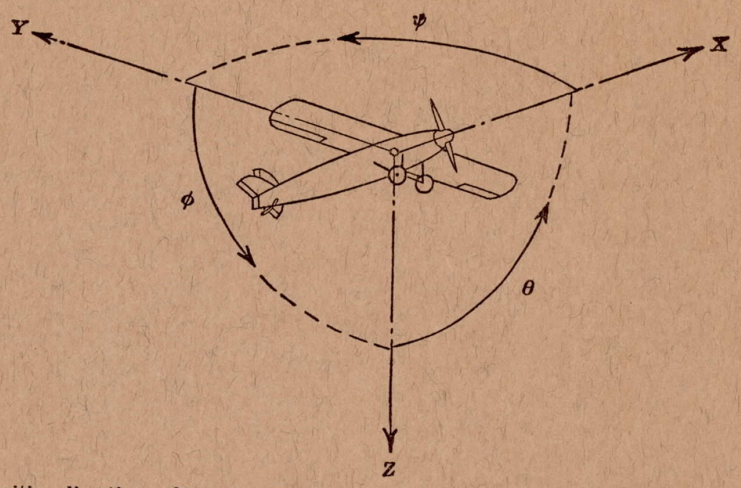

Positive directions of axes and angles (forces and moments) are shown by arrows

Axis		Force (parallel to axis) symbol	Moment about axis			Angle		Velocities	
Designation	Symbol		Designation	Symbol	Positive direction	Designation	Symbol	Linear (component along axis)	Angular
Longitudinal	X	X	Rolling	L	$Y \longrightarrow Z$	Roll	ϕ	u	p
Lateral	Y	Y	Pitching	M	$Z \longrightarrow X$	Pitch	θ	v	q
Normal	Z	Z	Yawing	N	$X \longrightarrow Y$	Yaw	ψ	w	r

Absolute coefficients of moment

$C_l = \frac{L}{qbS}$ (rolling) $\quad C_m = \frac{M}{qcS}$ (pitching) $\quad C_n = \frac{N}{qbS}$ (yawing)

Angle of set of control surface (relative to neutral position), δ. (Indicate surface by proper subscript.)

4. PROPELLER SYMBOLS

D, Diameter

p, Geometric pitch

p/D, Pitch ratio

V', Inflow velocity

V_s, Slipstream velocity

T, Thrust, absolute coefficient $C_T = \frac{T}{\rho n^2 D^4}$

Q, Torque, absolute coefficient $C_Q = \frac{Q}{\rho n^2 D^5}$

P, Power, absolute coefficient $C_P = \frac{P}{\rho n^3 D^5}$

C_s, Speed-power coefficient $= \sqrt[5]{\frac{\rho V^5}{P n^2}}$

η, Efficiency

n, Revolutions per second, r.p.s.

Φ, Effective helix angle $= \tan^{-1}\left(\frac{V}{2\pi r n}\right)$

5. NUMERICAL RELATIONS

1 hp. = 76.04 kg-m/s = 550 ft-lb./sec.
1 metric horsepower = 1.0132 hp.
1 m.p.h. = 0.4470 m.p.s.
1 m.p.s. = 2.2369 m.p.h

1 lb. = 0.4536 kg.
1 kg = 2.2046 lb.
1 mi. = 1,609.35 m = 5,280 ft.
1 m = 3.2808 ft.